Two-photon fluorescence cross-correlation spectroscopy as a potential tool for high-throughput screening of DNA repair activity

Maddalena Collini[1,3], Michele Caccia[1], Giuseppe Chirico[1,3], Flavia Barone[2], Eugenia Dogliotti[2] and Filomena Mazzei[2,*]

[1]Department of Physics, University of Milano-Bicocca, Piazza della Scienza 3, 20126 Milan, Italy, [2]Department of Environment and Primary Prevention, Istituto Superiore di Sanità, Viale Regina Elena 299, 00161 Rome, Italy and [3]CNR-INFM, Genoa, Italy

ABSTRACT

Several lines of evidence indicate that differences in DNA repair capacity are an important source of variability in cancer risk. However, traditional assays for measurement of DNA repair activity in human samples are laborious and time-consuming. DNA glycosylases are the first step in base excision repair of a variety of modified DNA bases. Here, we describe the development of a new sensitive DNA glycosylase assay based on fluorescence cross-correlation spectroscopy (FCCS) with two-photon excitation. FCCS was applied to the measurement of uracil DNA glycosylase activity of human cell extracts and validated by comparison with standard gel electrophoresis assay. Our results indicate that FCCS can be adapted to efficient assays for DNA glycosylase activity in protein extracts from human cells. This method has a potential for the development of automated screening of large number of samples.

INTRODUCTION

The cellular genome is exposed to various sources of damage such as UV and ionizing radiation, and to alkylating agents and reactive oxygen species owing to environmental stress and natural metabolic processes. To remove such damage and restore the integrity of the genome, specific DNA repair pathways have evolved, including base excision repair (BER), nucleotide excision repair (NER) and mismatch repair (MMR). The importance of DNA repair pathways is illustrated by the hereditary diseases xeroderma pigmentosum and hereditary non-polyposis colo-rectal cancer characterized by defects in NER and MMR, respectively, and high predisposition to

cancer [reviewed in (1)]. The biological consequences of persisting DNA damage might account also for the association between variation in DNA repair activities and population disease susceptibility. Convincing examples are the association between reduced DNA repair capacity (DRC) of UV damage and early occurrence of basal cell carcinomas (2) and reduced repair of benzo(*a*)pyrene DNA adducts and lung (3) and breast (4) cancer risk. The method used to measure DNA repair in these studies is the host–cell reactivation assay that is based on the expression of a reporter gene from a plasmid that is treated with a DNA-damaging agent *in vitro* and then introduced into the cells by transfection. The gene expression reflects the repair ability of the cells. However, this method is very laborious, time-consuming and subjected to assay variability. Other technical approaches involve the treatment of the cells with a DNA-damaging agent and then the analysis of DRC by using generalized methods to measure DNA single-strand breaks, like the comet assay [reviewed in (5)] or immunofluorescence detection of DNA adducts (6). The drawback of this approach is that DRC can be affected by cell exposure to DNA-damaging agents. More recently, population-based studies have been conducted by measuring the activity of a specific DNA repair enzyme in protein extracts from human cells. For instance, tobacco smoke induces the formation of oxidative damage that is primarily repaired by BER. The activity of the specific DNA *N*-glycosylase that initiates repair of 8-oxoguanine, OGG1, was measured in extracts of peripheral lymphocytes and an association between low levels of OGG1 and increased risk of lung cancer in smokers was reported (7,8).

DNA *N*-glycosylases are the enzymes that initiate BER by cleaving the N-glycosidic bond of the modified base and thus generating an apurinic/apyrimidinic (AP) site. BER is the major pathway that protects cells from nucleotide base damage. Therefore, it is of great interest to develop an assay that is

amenable to rapid and reproducible measurement of DNA glycosylase activities in human cell extracts to be used in molecular epidemiology studies.

Current assays for DNA glycosylases generally involve the use of radioactively labelled DNA substrates and are based on gel electrophoresis. This makes difficult to automate the assay for high-throughput screening of DRC. In this work we have explored the potential use of fluorescence cross-correlation spectroscopy (FCCS) to monitor DNA glycosylase activities in human cell extracts.

The FCCS method allows very sensitive detection of molecular dissociations. It is based on the computation of the cross-correlation of the fluctuations in the fluorescence emission of two spectrally distinct dyes that label the two molecular species. Since FCCS is based on the detection of the fluorescence fluctuations, the samples are tiny volumes at nanomolar concentration. A maximum cross-correlation is measured for non-dissociated samples for which the diffusion of both dyes through the excitation volume occur simultaneously. Upon dissociation the degree of cross-correlation decreases owing to the independent random passage of the two dyes through the excitation volume.

FCCS technique has been successfully applied to DNA hybridization (9), protein aggregation (10) and enzymatic assay (11–14). Other recent applications concern the use of the method as rapid assay (13,15) for kinetic reactions in homogeneous sample solutions.

Here, we report for the first time the successful use of the FCCS method to measure uracil DNA glycosylase (UDG) activity in human cell extracts. As a first example, a 30 bp long oligonucleotide, labelled with two spectrally distinct dyes at the 5′ and 3′ ends of the same strand, containing also a single uracil, was used as a probe. The recording of the coordinated spontaneous fluorescence fluctuations of the two dyes could allow us to verify the existence of physical linkage between the two fluorophores after the enzymatic reaction and then the entity of cleavage.

FCCS methodology was validated by a direct comparison with the traditional gel electrophoretic assay of UDG activity. A simulation study of the statistical requirements needed to reduce the acquisition time of the FCCS correlation functions indicates that FCCS has the potential to be an efficient tool for screening of large number of samples.

MATERIALS AND METHODS

Oligonucleotides

High-performance liquid chromatography-purified 30mer oligonucleotides 5′-GCGTAGAGCATTGTUATCCGAGCGT-CAGCG–3′, containing a single uracil and labelled at the 5′ end with Rhodamine green (RG) and/or at the 3′ end with Texas red (TR) were purchased from Thermo Electron (Thermo Electron GmbH, Germany). Unlabelled oligonucleotides (Invitrogen Corporation, CA) were purified before using by PAGE (16). The 30-mers were annealed to the complementary strand by heating at 90°C for 10 min, followed by a slow cooling at 4°C. The formation of duplex oligonucleotides was checked by electrophoresis on 15% polyacrylamide gels, run at 100 V for 16 h, at 4°C. Radioactive 5′ end labelling of the 30mer containing a single uracil was performed by

$[\gamma\text{-}^{32}P]ATP$ (Perkin Elmer, Italy) and T4 polynucleotide kinase (Boehringer-Mannheim, GmbH, Germany). ^{32}P-end labelled oligonucleotides were purified by Sephadex G-25. The annealing with the unlabelled complementary strands was performed as described above. A + G sequence reaction was performed according to the single reaction method developed by Negri *et al.* (17).

HeLa cell extract preparation and enzymatic digestion conditions

HeLa cells were collected in exponential growth phase and cell extracts were prepared as described previously (18). Briefly, 10^6 cells were resuspended in 20 µl of Buffer I (10 mM Tris–HCl, pH 7.8 and 200 mM KCl) and an equal volume of Buffer II was added (10 mM Tris–HCl, pH 7.8, 200 mM KCl, 2 mM EDTA, 40% glycerol, 0.2% NP-40, 2 mM DTT, 0.5 mM phenylmethylsulfonyl fluoride, 10 µg/ml aprotinin, 5 µg/ml leupeptin and 1 µg/ml pepstatin). The cell suspension was rocked at 4°C for 1 h and then centrifuged at 16 000 g for 10 min. Total protein concentration was measured by standard Bradford assay.

5′-^{32}P-end labelled or fluorescently double labelled oligonucleotides, containing a single uracil lesion, were incubated with increasing amount of HeLa cell extracts (up to 200 ng) in 10 µl of 70 mM HEPES–KOH, pH 7.8, 3 mM $MgCl_2$ and 1 mM Na_2EDTA buffer. Cold duplex substrate was also added to the ^{32}P reaction mixture to make the radioactive and fluorescent samples digestion conditions completely superimposable. Reactions were stopped by EDTA addition up to 10 mM final concentration. In order to separate the strands and reveal chain breakage, the samples were then heated at 90°C for 5 min and quickly cooled.

Gel electrophoresis assay

The cleavage products, obtained by the ^{32}P-end labelled samples digestion, were electrophoresed on 20% denaturing polyacrylamide–urea gel made in TBE buffer and run at 500 V for 1 h 40 min. Autoradiograph scans were performed by an ULTROSCAN XL laser densitometer (Pharmacia LKB Biotechnology AB, Sweden) and the Image Master software (Pharmacia LKB Biotechnology AB, Sweden). Band area evaluation was performed by using the NIH public domain software available on the Internet at http://rsb.info.nih.gov/nih-image/.

FCCS set-up and fluorescence assay

The laser source was a mode-locked Ti:Sapphire laser (Tsunami 3960, Spectra Physics, CA) pumped by a solid-state laser at 532 nm (Millennia V, Spectra Physics, CA) that produces pulses with $\cong$200 fs FWHM on the sample plane (19,20), with repetition frequency of 80 MHz and average power output of ∼10 mW at $\lambda_{exc} = 830$ nm at the focal plane. The pulse width was measured by an optical interferometer method that exploit the two-photon fluorescence emission of a concentrated solution of dye on the focal plane of the microscope, as detailed in ref. (20). The average power on the focal plane has been estimated by means of a $\cong$2 cm wide power meter right above the wide numerical aperture objective with water index matching.

The optical set-up was built around an inverted microscope (TE300; Nikon, Japan). A portion of the laser beam was sent to the epifluorescence port of the microscope and was reflected by a dichroic mirror (650 DCSPRX C72-38; Chroma Inc., Brattleboro, VT) into the objective (NA = 1.2, Plan Apochromat ×60 water immersion; Nikon, Japan). The entrance pupil of the objective was slightly underfilled in order to reach excitation volumes $\cong 0.3$ μm^3. The two-photon excitation fluorescence signal, coming from TR and RG, was collected by the objective, filtered through a short-pass 670 nm filter (Chroma Inc.) and splitted by a dichroic filter (595 nm; Chroma Inc.). The splitted fluorescence signal was focussed on two avalanche photodiodes (APD) (SPCM-AQR-14; Perkin Elmer, Wiesbaden, Germany) mounted at right angle. TR and RG showed an emission peak, respectively, at $\lambda_{em} = 612$ nm and $\lambda_{em} = 532$ nm, thereby allowing an easy spectral discrimination by means of band pass filters (12). Moreover, no Förster resonance energy transfer between RG and TR was expected owing to a poor superposition of the RG emission and TR single-photon absorption bands (for TR $\lambda_{ex} = 591$ nm). In order to further enhance the separation between the green and the red channel emission, a 535/50 nm band pass filter was positioned in front of the APD in the RG detection channel, whereas a 645/74 nm (Chroma Inc.) was mounted in the TR detection channel. In this way, the dyes crosstalk could be minimized [see discussion and ref. (21)].

The photon-count signal coming from the two APDs was sent to ALV5000 (ALV, Langen, Germany) correlator board in order to compute the fluorescence autocorrelation and cross-correlation functions with minimum lag time of 200 ns.

As suggested by Heinze *et al.* (21), 50 nM Rhodamine 6G solutions in ethanol (diffusion coefficient $D = 300$ $\mu m^2/s$) was used as system calibration standard for the day-to-day estimation of the excitation volume. A global fitting of the Rhodamine 6G autocorrelations on the green and the red channel together with the pseudo-cross-correlation functions yielded the same value of the beam waist, within experimental error. This result testified that the excitation volume seen by both channels was the same, equal to $V_{exc} \cong 0.3 \pm 0.03$ μm^3. Measurements repeated on samples at concentrations in the range 20–200 nM gave very similar results, within $\cong 10\%$ uncertainty.

The cleavage products, obtained by the digestion of the double labelled fluorescent samples, as described in Materials and Methods, were diluted to the final dye concentration of 150 nM. FCCS measurements were carried out in 200 μl wells (Lab-Tek™ chambered cover glass, 8 wells; NALGE-NUNC, Rochester, NY). All the FCCS measurements were performed with excitation at $\lambda_{ex} = 830$ nm, where both dyes show a good two-photon excitation cross-section (21), at 23°C. Typically, 5–20 correlations functions were collected for a total measurement time ranging from 5 to 20 min depending on the fluorescence rate. Single labelled samples with either RG or TX at one end were employed to estimate the crosstalk between the green and the red detection channel in our set-up.

The samples to be analysed by FCCS were also run on 20% polyacrylamide–urea gel made in TBE buffer at 40 W for 2 h. Fluorescence scans were performed directly on the gel using Typhoon 9200 Gel Imager (Amersham Biosciences Europe,

GmbH, Germany) and images displayed by means of ImageQuant software (Amersham Biosciences Europe, GmbH, Germany).

FCCS data analysis

We report here the basic equations needed for FCCS data analysis, referring to specific literature (21) for further details. The auto (G_{XX} and G_{YY}) and cross-correlation (G_{XY}) functions of the fluorescence signal detected through the green, $F_G(t)$, and the red, $F_R(t)$, channels were computed as follows:

$$G_{XY}(\tau) = \frac{\langle F_X(t+\tau)F_Y(t)\rangle_t - \langle F_X(t)\rangle_t \langle F_Y(t)\rangle_t}{\langle F_X(t)\rangle_t \langle F_Y(t)\rangle_t} \qquad \mathbf{1}$$

where X, Y stand for G (Rhodamine green channel) or R (Texas red channel). When no crosstalk was present from the green to the red channel, the correlation function was computed as follows:

$$G_{XY}(\tau) = G_{XY}(0)\left(\frac{1}{1+\frac{\tau}{\tau_D}}\right)\left(\frac{1}{1+\frac{\tau}{\tau_Z}}\right)^{0.5} \qquad \mathbf{2}$$

where τ_D and τ_Z are the diffusion times in the focal plane and along the optical axis of the microscope. Here, it is assumed that crosstalk may occur only from the green to the red channel, since emission is always red-shifted with respect to excitation. The double (GR) and single labelled DNAs (G and R) species occur in the excitation volume in average numbers, $\langle N_{GR}\rangle$, $\langle N_G\rangle$ and $\langle N_R\rangle$, respectively. The information on the number of molecules of these species is embedded in the value of $G_{XY}(0)$ as follows:

$$G_{GG}(0) = \frac{\gamma}{\langle N_G + N_{GR}\rangle}$$

$$G_{RR}(0) = \frac{\gamma}{\langle N_R + N_{GR}\rangle} \qquad \mathbf{3}$$

$$G_{GR}^0(0) = \frac{\gamma \langle N_{GR}\rangle}{\langle N_G + N_{GR}\rangle \langle N_R + N_{GR}\rangle}$$

where $\gamma = 0.076$ (22,23) for the case of two-photon excitation fluorescence spectroscopy. The Equation 3 requires (i) an axially symmetric Gaussian–Lorentzian excitation volume profile, (ii) an equal value of the molecular brightness (the absorption cross-section times the quantum yield) on both channels for the singly and the doubly labelled species and (iii) the absence of crosstalk from the green to the red channel (no crosstalk from the red to the green channel is ensured by the Stokes shift of the emission with respect to the excitation). The average number of molecules of any of the three species is related to its average concentration and to the excitation volume as follows: $C_X = \langle N_X\rangle/V_{EXC}$. The amplitude of the cross-correlation function depends linearly on the number of doubly labelled molecules, $\langle N_{GR}\rangle$, only if $\langle N_{GR}\rangle \gg \langle N_R\rangle,\langle N_G\rangle$.

However, the concentration of the doubly labelled species can always be obtained as

$$C_{GR} = \frac{G_{GR}(0)}{G_{RR}(0)G_{GG}(0)}\frac{\gamma}{V_{EXC}}. \qquad \mathbf{4}$$

When a substantial contribution from crosstalk is present on

the red channel, a cross-correlation term is present (even when $\langle N_{GR} \rangle = 0$), and amounts to

$$G_{GR}^x(0) = \left(\frac{\gamma}{\langle N_G \rangle + \langle N_{GR} \rangle}\right)\frac{\xi_T}{100 + \xi_T} \qquad \textbf{5}$$

where ξ_T is the crosstalk percentage related to the molecular brightness of the singly labelled red and green species on the red channel, ε_R^r and ε_G^r, as $\xi_T = 100\varepsilon_G^r/\varepsilon_R^r$. Clearly, when no crosstalk is present, i.e. $\xi_T \rightarrow 0$, then the residual cross-correlation $G_{GR}^x(0)$ vanishes. However, the true cross-correlation $G_{GR}^0(0)$ is computed by subtracting Equation 5 from the extrapolation of the measured cross-correlation function, $G_{GR}(0)$. The extrapolation of the auto- and cross-correlation functions were obtained by non-linear fitting of the experimental functions to Equation 2, and by keeping the diffusion coefficient, D, of the DNA fragment and the $G_{GR}(0)$ value as free parameters of the fit. The in-plane diffusion time τ_D was computed according to the measured laser beam waist, w_0 as $\tau_D = w_0^2/8D$. The ratio τ_D/τ_Z was estimated by approximating the Gaussian–Lorentzian shape of the excitation volume to a 3D-Gaussian shape from which we obtain that $\tau_D/\tau_Z \cong \lambda^2/(2\pi^2 w_0^2) \cong 0.12$ (assuming $\lambda = 830$ nm and $w_0 \cong 0.53$ μm). This value was kept fixed in fitting the FCCS correlation functions.

RESULTS

Assay of UDG activity by gel electrophoresis analysis

In order to validate the FCCS assay to detect DNA glycosylase activity of human cell extracts, we compared this new methodology with the standardized gel electrophoresis assay involving a radiolabelled DNA substrate. As a model system we selected the UDG activity assay. The DNA strand containing the uracil residue was radiolabelled with ^{32}P at the 5′ end (Figure 1A). UDG is expected to remove the uracil leading to the formation of an abasic site. This site is then cleaved by the major 5′ AP endonuclease present in the protein extract. The cleaved DNA fragments can be resolved by denaturing PAGE and the radiolabelled fragments can be distinguished by size. The uncleaved fragment will run as a 30mer oligonucleotide, whereas the detectable cleavage product is a 14mer. Figure 1B shows a typical gel pattern of the enzymatic reaction products. The extent of cleavage was measured by densitometric analysis of the autoradiography. The decrease in the percentage amount of the intact DNA moiety was observed at increasing HeLa cell extracts up to 200 ng (Figure 1C). The linear portion of the curve is shown in the inset of Figure 1C.

Assay of UDG activity by FCCS

The application of FCCS for quantitative analysis requires that (i) the excitation and observation volumes are the same for the two dyes and (ii) the crosstalk (i.e. the leakage signal from one dye to the complementary channel) is barely detectable. Dual color excitation, as used in most of the FCCS applications (11–14), involves the use of two different laser sources that are focussed at distinct positions in the sample, owing to chromatic aberrations of the microscope objective. Here, we use a non-linear (two-photon) excitation that allows the excitation
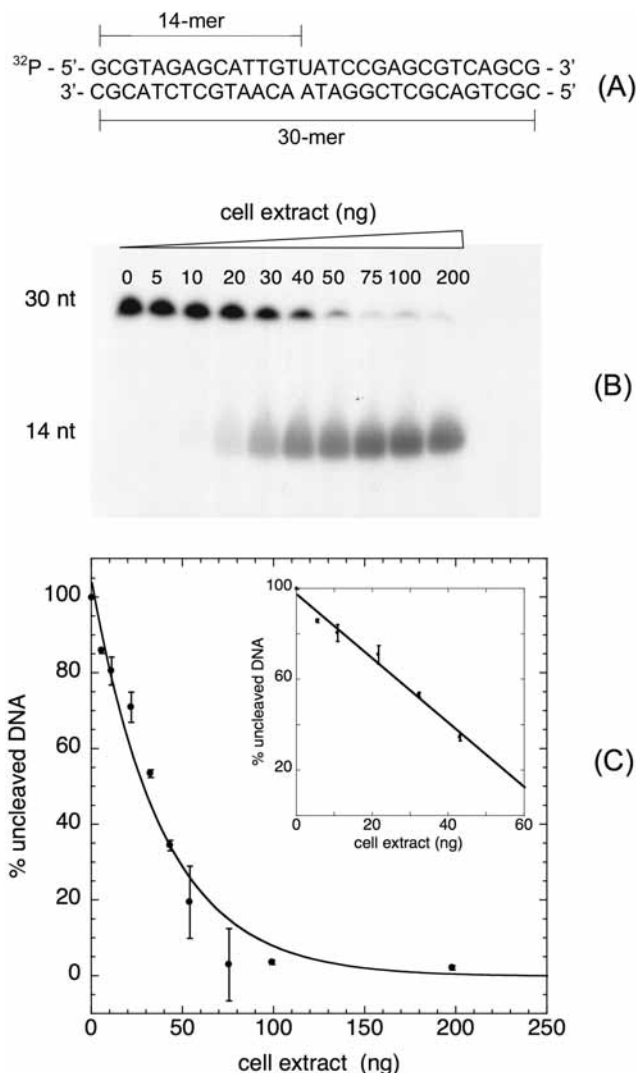

Figure 1. (**A**) Sequence of the ^{32}P end-labelled DNA substrate. The 14mer fragment produced by the UDG incision is shown. (**B**) Autoradiograph of the gel where the UDG cleavage products were run. The upper wedge indicates the increasing amount of HeLa cell extracts in ng. (**C**) Results of the densitometric analysis. The mean of three independent experiments has been reported as percentage of the uncleaved fraction versus the HeLa cell extract amount in ng. The final reaction volume being 10 μl. Inset: linear portion of the same plot.

of both dyes at the same infrared wavelength (21). This method ensures similar excitation volumes for the two dyes, thus avoiding optical corrections of the objective aberrations. The superposition of the observation volumes observed through the green and the red channels was checked by changing the collection optics of one of the two detectors in order to maximize the superposition of the auto- and cross-correlation functions for a sample with a single reference dye. As shown in Figure 2A, the autocorrelation functions, on the green and the red channels, of the fluorescence emission of a sample of Rhodamine 6G were found in excellent agreement with the pseudo-cross-correlation function between the green and the red channel. In this case, the cross-correlation arises from the almost equal ratio of the signal of the Rhodamine 6G in the green and red channels. The close matching of the
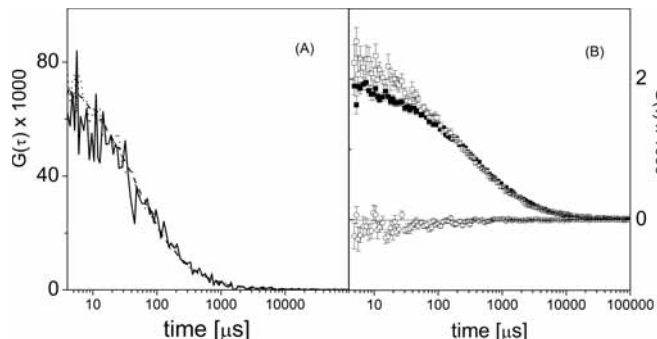
Figure 2. (**A**) Autocorrelation functions on the green (solid line) and red channels (dashed line) and cross-correlation function (dotted line) of a 50 nM Rhodamine 6G sample in ethanol. Excitation wavelength was 830 nm, excitation intensity was about 60–120 kW/cm^2. (**B**) Autocorrelation functions of singly labelled DNA fragments on the green (RG, open squares) and red (TR, closed squares) channels. Cross-correlation of a 1:1 mixture of singly labelled fragments (open circles). In both cases the signals were splitted by a dichroic mirror (595 nm) and further selected by an emission filter at 532 ± 25 nm (RG channel) or an emission filter 640 ± 37 nm (TR channel).
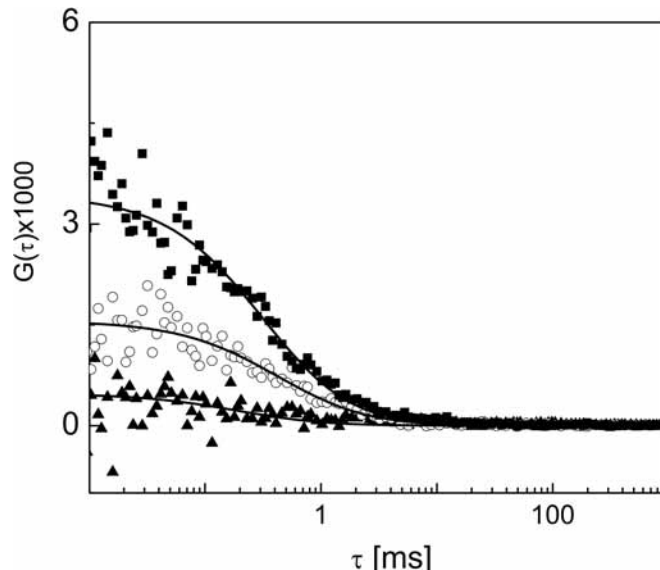

Figure 3. Cross-correlation functions of doubly labelled DNA fragments solutions [(DNA) = 150 nM] previously incubated with increasing amount of HeLa cell extracts: 0 (closed square), 43 (open circle) and 100 ng (closed triangle) in a final volume of 10 μl. Solid lines are the best fit to the Equation 2 of the text.

auto- and the cross-correlation functions proves that we are observing the same volume in the sample on both channels.

We then estimated the amount of crosstalk for the 30 bp oligonucleotides used as DNA substrate in our DNA glycosylase assay. Figure 2B shows that the autocorrelation functions of two equal concentration solutions of 30 bp oligonucleotides, single labelled either with TR (closed squares) or RG (open squares), are in very good mutual agreement down to 0.1 ms of lag time. For shorter lag times a fast triplet component is more evident for RG than for TR. The cross-correlation function is then collected from a 1:1 mixture of the two solutions of singly labelled 30 bp DNAs. In this case, no true cross-correlation is expected as confirmed by the almost flat cross-correlation function shown in Figure 2B. This behaviour is owing to the very low amount of crosstalk of the RG labelled DNAs into the TR channel, $\varepsilon_G^r \cong 0.2$ kHz. compared with the molecular brightness of the singly labelled TR fragments in the red channel, $\varepsilon_R^r \cong 6.5$ kHz. For comparison, the molecular brightness of the singly labelled RG fragments in the green channel is $\varepsilon_G^g \cong 1.4$ kHz, owing to an about 3-fold dynamic quenching of the dye by a close guanine base. This corresponds to a crosstalk percentage $\xi_T \cong 3\%$. Owing to this very low value of ξ_T, the cross-correlation functions were not corrected for crosstalk.

The FCCS cleavage assay is based on the measurement of the amplitude of the FCCS function at zero lag time. Figure 3 reports the cross-correlation functions for a series of DNA samples previously incubated with increasing amount of HeLa cell extracts. The amplitude of the cross-correlation functions becomes progressively lower by increasing the HeLa extracts concentration. According to Equation 3, this suggests a progressive reduction of the doubly labelled species. In fact, the value of $G_{GR}(0)$ is proportional to the concentration of the doubly labelled sample (21), since the total amount of red and green dyes is constant during the cleavage assay.

The diffusion coefficient, estimated directly from the cross-correlation functions for a protein amount <20 ng, is $D = 95 \pm 20$ μm^2/s, in good agreement with the value of

90 μm^2/s, as expected for a 30 base oligomer (24). When fitting the autocorrelation functions, the diffusion coefficient is the same as that found in the cross-correlation case at low enzyme concentrations, whereas it increases up to a value $D = 140 \pm 40$ μm^2/s at the highest enzyme concentrations tested. This value is close to that expected for a 14 base oligomer (130 μm^2/s), thus confirming that under these experimental conditions the large majority of uracil-containing oligonucleotides are cleaved. The diffusion coefficient, measured from the time decay of the autocorrelation function, could then be taken as a measure of DNA cleavage, provided that a linear interpolation between the diffusion coefficient of the cleaved and uncleaved DNA is assumed. In the present case, however, the diffusion coefficients of the two cleaved fragments are too close (only a factor $\cong 1.5$) to allow quantitative analysis of enzyme activity to be performed in this way. An appropriate design of the DNA substrate (cleavage products clearly differentiated by size) would allow to use the diffusion coefficient to monitor the occurrence of specific enzymatic reactions in the test tube.

We evaluated the crosstalk correction to $G_{GR}(0)$ from Equations 4 and 5 and the statistical uncertainty on $G_{GR}(0)$ from those of the auto- and cross-correlation functions (25). As shown in Figure 4, the correction is largely affected by the crosstalk percentage, ξ_T, especially at low uncleaved DNA fractions, $\alpha = \langle N_{GR} \rangle / (\langle N_R \rangle + \langle N_G \rangle + \langle N_{GR} \rangle)$. In the present case, $\xi_T \cong 3\%$, the correction needed is <4% at $\alpha = 0.7$ (see inset of Figure 4). As described above, such small crosstalk percentage is also owing to a 3-fold quenching of the RG dye by adjacent DNA bases. Not only an unquenched dye would have yielded smaller uncertainties on $G_{GR}(0)$ but also larger corrections ($\cong 33 \pm 10\%$) owing to a larger crosstalk percentage ($\xi_T \cong 10\%$). The present case seems to be a reasonable compromise between large molecular brightness and low crosstalk.
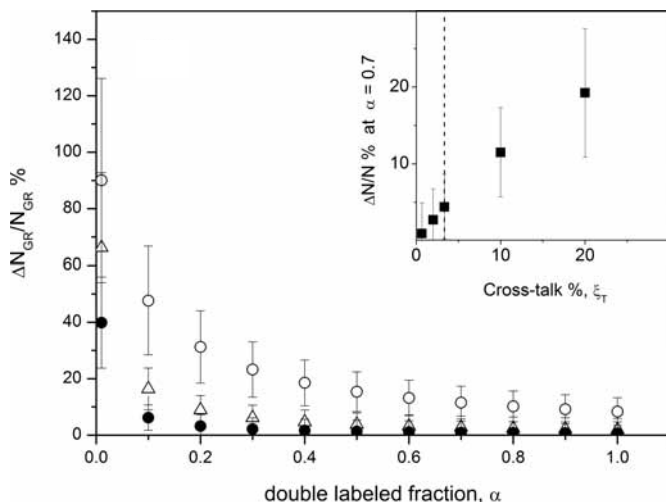
Figure 4. Percent correction to be applied to the measured number of uncleaved DNA fragments per excitation volume, $\Delta N_{GR}/N_{GR}\%$, owing to the crosstalk of the green to the red channel, versus the fraction of uncleaved DNA fragments. Symbols refer to $\xi_T = 10\%$ (open circles), 2% (open triangles) and 0.7% (closed circles). Inset: $\Delta N_{GR}/N_{GR}\%$ at $\alpha = 0.7$ versus the crosstalk percentage, ξ_T. The dashed vertical line indicate $\xi_T = 3\%$.
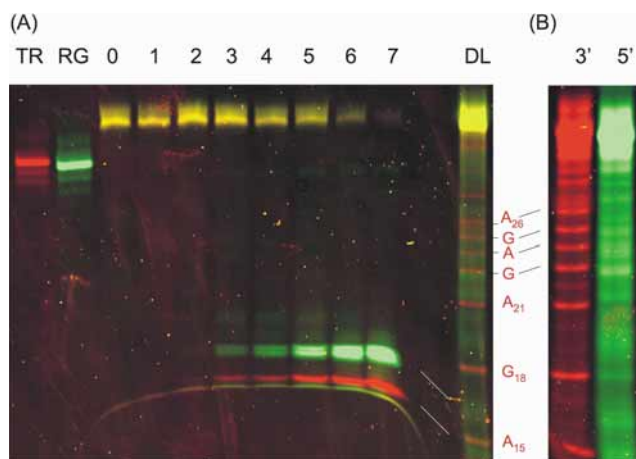

Figure 5. (**A**) Denaturing gel electrophoresis pattern of the cleavage reaction products. The same double labelled duplexes used for FCCS experiments are run. (A) TR, single labelled Texas red-30mer; RG, single labelled Rhodamine green-30mer; lanes 0–7, double labelled DNA reacted with 0, 5, 11, 21, 32, 43, 100, 200 ng of HeLa cell extracts. The uncleaved fragments reveal the co-migration of the two colors (yellow band). Lane DL, A + G reaction on the double labelled strand. (**B**) A + G reaction on single labelled oligonucleotides (3′ end, Texas red; 5′ end, Rhodamine green). Bases are always numbered from the 5′ end.

The presence in the reaction mixture of exclusively double labelled duplex substrates was verified by gel electrophoresis analysis of the FCCS samples (Figure 5). No contaminating single labelled oligonucleotides were detected (compare lanes TG and TR with lanes 0–7). Figure 5 shows that the use of a substrate labelled at both 5′ and 3′ ends allows to monitor the formation of both cleavage products (14mer and 15mer), if high voltage gel electrophoresis is employed. The decrease of the intensity of the yellow band, corresponding to full-length double labelled oligonucleotides, paralleled the increase in the yield of green and red fragments (14mer and 15mer), as expected by enzymatic cleavage of the U-containing duplexes. The
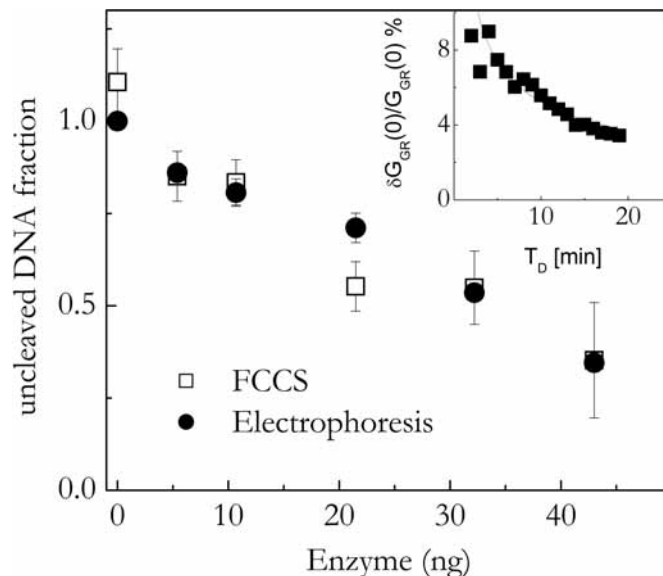

Figure 6. Comparison of the FCCS to the electrophoresis assay. Closed circles are the fraction of the uncleaved DNA fragments obtained from digestion with the HeLa cell extracts as measured by autoradiograph, open squares are from FCCS assay. Open squares are the estimates obtained from the cross-correlation amplitude extrapolated to zero lag time. The reference concentration for both sets is the one (150 nM) of the sample analysed by electrophoresis at 0 enzyme concentration. Bars indicate standard errors. Inset: percent standard error on the best fit cross-correlation data at zero delay time, $G_{GR}(0)$, versus the experiment duration, T_D. The fitting of the cross-correlation functions has been performed by keeping the diffusion coefficient D constant to the value of the 30mer DNA. The solid line is a best fit with the function $\approx T_D^{-0.5}$.

correct assignment of the bands was verified by A + G sequencing reactions (Figure 1A, lane DL and Figure 1B) (17). The slower electrophoretic mobility of the green 14mer as compared with the red 15mer is most probably due to the absence of a terminal PO_4 group in the shorter fragments (26).

Figure 6 shows the comparison of the gel electrophoresis (Figure 1) and FCCS results obtained by performing the cleavage reaction under the same experimental conditions. The superimposition of the data testified that FCCS could be successfully applied to detection of DNA glycosylase activity in human cell extracts.

The main issue was then to estimate how much it was possible to reduce the detection time of the enzymatic reaction efficiency by FCCS. To this purpose, we made a statistical analysis of the cross-correlation functions with increasing experimental durations, from $T_D = 2$ to $T_D = 20$ min per correlation function. The percentage uncertainty on the extrapolation of the cross-correlation function, reported in Figure 6 (inset), scales very well as $T_D^{-0.5}$, as expected for perfect Poissonian distributions. This analysis indicates that by decreasing the experimental duration from 20 to 5 min, per cross-correlation function, the experimental uncertainty raises only from $\cong 4\%$ to $\cong 7\%$. This implies that the reduction of the detection time is feasible and makes this method applicable to high throughput screening.

DISCUSSION AND CONCLUSIONS

In this study, we show the successful application of fluorescence spectroscopy correlation technique to DNA glycosylase

assays of human cell extracts and we propose this method as an efficient tool for screening of DNA repair activity of a large number of samples. We provide evidence that the concentration of highly diluted solutions of double labelled DNA fragments can be estimated from the analysis of the correlated fluorescence fluctuations of the two fluorophores. We show that an intact DNA sample, containing a lesion of interest, labelled with two dyes on the same strand causes a maximal correlation of the fluorescence emission of the two dyes. As the DNA glycosylase cleavage reaction occurs, a decrease in the correlation of the two dyes emission is observed. It is worthwhile to notice that, by FCCS application, the level of glycosylase activity in cells was unambiguously detected without the separation of intermediate digestion products. Moreover, an alternative design of the oligonucleotide sequence and of the uracil position could easily allow us to perform a real-time detection of the lesion excision, avoiding the heating step performed to reveal the single-strand break.

The comparison of this technique with the traditional gel electrophoresis assay, reported in Figure 6, confirms that the two methods detect the same amount of cleaved DNA and thus the same DNA glycosylase activity of the test protein extracts. The agreement is particularly good all the way up to an enzyme concentration $\cong 5$ ng/μl (50 ng total amount) that corresponds to a fraction of uncleaved DNA $\cong 25\%$. This is the relevant range of concentrations for evaluation of DNA repair activity since within this range the amount of cleavage is linear in relation to protein concentration within the reaction mixture (Figure 1C).

The measurement of DNA glycosylase activity by using a radioactively labelled DNA substrate containing the lesion of interest and gel electrophoresis analysis of the cleavage products has been largely applied in the past. This method provides a measure of DNA glycosylase activity from the distribution of the substrate DNA molecules between the cleaved and uncleaved products (Figure 1). This experiment can be implemented on tens of samples at the same time. The reading implies the computation of the ratio of the amount of DNA in two well distinct bands. This assay is, however, time-consuming. A complete run of the experiments lasts for $\sim$16–24 h, so that the method is hardly applicable to the analysis of large amount of samples in a relatively short time, as expected in a screening assay. Moreover, the use of radioactivity involves a short lifetime of the DNA probe. Last but not the least, protection procedures need to be implemented to reduce the risk associated with radiation exposure. The use of photostimulable storage phosphor technology, as well as the alternative DNA labelling with fluorescent dyes, has been shown to greatly reduce the risks, but not the time. These latter methods are also based on gel electrophoresis, so that the difficulty to automate the assay for large-scale experiments still remains. It would be, therefore, desirable to reduce the time length of the experiment and increase the maximum number of samples that can be analysed simultaneously. The possibility to reduce the time acquisition in FCCS assay was investigated by a simulation study. A time acquisition of 5 min, per cross-correlation function, was found associated to the percentage uncertainty on the extrapolation of the cross-correlation function of $\sim$7%. This latter value, as shown also by the comparison of gel electrophoresis and FCCS

results, assures that DNA cleavage reaction can be correctly monitored.

With a minimum acquisition time $T_D \cong 5$ min per correlation function on an average number of molecules per excitation volume equal to $\sim$15, and acquiring two cross-correlation functions per sample, a total of $\sim$6 samples per hour could be processed. Additional technical improvements can be obtained by decreasing to 30 μl the sample volume and increasing the excitation volume of one order of magnitude by reducing of a factor $\cong 0.56$ the laser beam diameter at the entrance pupil of the microscope objective (the excitation volume scales as the fourth power of the laser beam waist). In this way a reduction up to 1/100 of the cell extract concentration could be applied. Therefore, this method fulfils the requirements of rapidity and sensitivity to be used for automatic sequential reading of the fluorescence cross-correlation and can be proposed for high-throughput screening.

REFERENCES

1. Hoeijmakers,J.H. (2001) Genome maintenance mechanisms for preventing cancer. *Nature*, **411**, 366–374.
2. Wei,Q., Matanoski,G.M., Farmer,E.R., Hedayati,M.A. and Grossman,L. (1993) DNA repair and aging in basal cell carcinoma: a molecular epidemiology study. *Proc. Natl Acad. Sci. USA*, **90**, 1614–1618.
3. Wei,Q., Cheng,L., Amos,C.I., Wang,L.E., Guo,Z., Hong,W.K. and Spitz,M.R. (2000) Repair of tobacco carcinogen-induced DNA adducts and lung cancer risk: a molecular epidemiologic study. *J. Natl Cancer Inst.*, **92**, 1764–1772.
4. Shi,Q., Wang,L.E., Bondy,M.L., Brewster,A., Singletary,S.E. and Wei,Q. (2004) Reduced DNA repair of benzo[*a*]pyrene diol epoxide-induced adducts and common XPD polymorphisms in breast cancer patients. *Carcinogenesis*, **25**, 1695–1700.
5. Berwick,M. and Vineis,P. (2000) Markers of DNA repair and susceptibility to cancer in humans: an epidemiologic review. *J. Natl Cancer Inst.*, **92**, 874–897.
6. Kennedy,D.O., Agrawal,M., Shen,J., Terry,M.B., Zhang,F.F., Senie,R.T., Motykiewicz,G. and Santella,R.M. (2005) DNA repair capacity of lymphoblastoid cell lines from sisters discordant for breast cancer. *J. Natl Cancer Inst.*, **97**, 127–132.
7. Paz-Elizur,T., Krupsky,M., Blumenstein,S., Elinger,D., Schechtman,E. and Livneh,Z. (2003) DNA repair activity for oxidative damage and risk of lung cancer. *J. Natl Cancer Inst.*, **95**, 1312–1319.
8. Gackowski,D., Speina,E., Zielinska,M., Kowalewski,J., Rozalski,R., Siomek,A., Paciorek,T., Tudek,B. and Olinski,R. (2003) Products of oxidative DNA damage and repair as possible biomarkers of susceptibility to lung cancer. *Cancer Res.*, **63**, 4899–4902.
9. Schwille,P., Meyer-Almes,F.J. and Rigler,R. (1997) Dual-color fluorescence cross-correlation spectroscopy for multicomponent diffusional analysis in solution. *Biophys. J.*, **72**, 1878–1886.
10. Bieschke,J., Giese,A., Schulz-Schaeffer,W., Zerr,I., Poser,S., Eigen,M. and Kretzschmar,H. (2000) Ultrasensitive detection of pathological prion protein aggregates by dual-color scanning for intensely fluorescent targets. *Proc. Natl Acad. Sci. USA*, **97**, 5468–5473.
11. Kettling,U., Koltermann,A., Schwille,P. and Eigen,M. (1998) Real-time enzyme kinetics of restriction endonuclease EcoRI monitored by dual-color fluorescence cross-correlation spectroscopy. *Proc. Natl. Acad. Sci. USA*, **95**, 1416–1420.

12. Rarbach,M., Kettling,U., Koltermann,A. and Eigen,M. (2001) Dual-color fluorescence cross-correlation spectroscopy for monitoring the kinetics of enzyme-catalyzed reactions. *Methods*, **24**, 104–116.

13. Kolterman,A., Kettling,U., Bieschke,J., Winkler,T. and Eigen,M. (1998) Rapid assay processing by integration of dual-color fluorescence cross-correlation spectroscopy: high throughput screening for enzyme activity. *Proc. Natl Acad. Sci. USA*, **95**, 1421–1426.

14. Jahnz,M. and Schwille,P. (2005) An ultrasensitive site-specific DNA recombination assay based on dual-color fluorescence cross-correlation spectroscopy. *Nucleic Acids Res.*, **33**, e60.

15. Winkler,T., Kettling,U., Koltermann,A. and Eigen,M. (1999) Confocal fluorescence coincidence analysis: an approach to ultra high-throughput screening. *Proc. Natl Acad. Sci. USA*, **96**, 1375–1378.

16. Sambrook,J., Fritsch,E.F. and Maniatis,T. (1989) *Molecular Cloning: A Laboratory Manual*. Cold Spring Harbor Laboratory Press, Cold Spring Harbor, NY.

17. Negri,R., Costanzo,G. and Di Mauro,E. (1991) A single-reaction method for DNA sequence determination. *Anal. Biochem.*, **197**, 389–395.

18. Biade,S., Sobol,R.W., Wilson,S.H. and Matsumoto,Y. (1998) Impairment of proliferative cell nuclear antigen-dependent apurinic/apyrimidinic site repair on linear DNA. *J. Biol. Chem.*, **273**, 898–902.

19. Cannone,F., Chirico,G. and Diaspro,A. (2003) Two-photon interactions at single fluorescent molecule level. *J. Biomed. Opt.*, **8**, 391–395.

20. Cannone,F., Chirico,G., Baldini,G. and Diaspro,A. (2003) Measurement of the laser pulse width on the microscope objective plane by modulated autocorrelation method. *J. Microsc.*, **210**, 149–157.

21. Heinze,K., Koltermann,A. and Schwille,P. (2000) Simultaneous two-photon excitation of distinct labels for dual-color fluorescence cross-correlation analysis. *Proc. Natl Acad. Sci. USA*, **97**, 10377–10382.

22. Berland,K.M., So,P.T. and Gratton,E. (1995) Two-photon fluorescence correlation spectroscopy: method and application to the intracellular environment. *Biophys. J.*, **68**, 694–701.

23. Schwille,P. (2001) Cross-correlation analysis in FCS. In Elson,E.L. and Rigler,R. (eds), *Fluorescence Correlation Spectroscopy. Theory and Applications*. Springer, Berlin, pp. 360–378.

24. Garcia de la Torre,J.G. and Bloomfield,V.A. (1981) Hydrodynamic properties of complex, rigid, biological macromolecules: theory and applications. *Q. Rev. Biophys.*, **14**, 81–139.

25. Koppel,D.E. (1974) Statistical accuracy in fluorescence correlation spectroscopy. *Phys. Rev. A*, **10**, 1938–1945.

26. Becerra,S.P., Detera,S.D. and Wilson,S.H. (1983) Anomalous electrophoretic migration of oligonucleotides with terminal –OH groups: applications for DNA exonuclease characterization. *Anal. Biochem.*, **129**, 200–206.